JOURNAL OF GEOPHYSICAL RESEARCH, VOL. 104, NO. C11, PAGES 25,821–25,831, NOVEMBER 15, 1999

Relationship between air-sea gas transfer and short wind waves

Erik J. Bock[1]
Woods Hole Oceanographic Institution, Woods Hole, Massachusetts

Tetsu Hara
Graduate School of Oceanography, University of Rhode Island, Narragansett

Nelson M. Frew and Wade R. McGillis
Woods Hole Oceanographic Institution, Woods Hole, Massachusetts

Abstract. Laboratory studies have been conducted in two circular wind wave flumes to investigate the relationship between air-sea transfer velocities of weakly soluble, nonreactive gases and wind-generated surface waves over clean water surfaces and in the presence of surface films. Detailed surface wave measurements have been made using a scanning laser slope gauge. In the circular tanks, longer gravity waves (wavenumber below 12 rad/m) are hardly affected by surfactant, while shorter waves (above 100 rad/m) are significantly reduced. With higher surfactant concentrations, waves above 200-300 rad/m may be completely eliminated. Because of the absence of narrow-banded fetch-limited gravity waves, the wave fields in the circular tanks are significantly different from those in linear wind wave flumes. At a given wind friction velocity, the transfer velocity may decrease by as much as 60% because of surface films. Regardless of the surfactant concentrations, the transfer velocity shows a reasonable correlation with the total mean square slope and with the mean square slope of shorter wind waves (wavenumber above 200 rad/m). However, it shows a poor correlation with the mean square slope of longer wind waves (wavenumber below 50 rad/m). These observations suggest that short wind waves play an important role in air-sea gas exchange.

1. Introduction

The accurate prediction of air-sea gas transfer velocity is crucial in estimating the global budget of various climatically important gases, including carbon dioxide, chlorofluorocarbons (CFCs), and dimethylsulfoxide (DMS). Our current knowledge of air-sea transfer velocities of weakly soluble, nonreactive gases is limited to empirical relationships between the mean wind speed and the gas transfer velocity [*Liss and Merlivat*, 1986; *Wanninkhof*, 1992]. These relationships were derived using tracer gases through mass balance techniques. These techniques require long averaging periods that tend to incorporate a great deal of wind variability within each estimate of the transfer velocity. Therefore it is not surprising that the scatter of this data is rather large, particularly because the results indicate that the transfer velocity is not a linear function of wind speed. Furthermore, the transfer velocity should depend not only on the wind speed but on other environmental parameters, such as wind waves, surface films, and subsurface turbulence.

In Figure 1 we represent the physical processes influencing the gas exchange by boxes and possible interactions among the processes by arrows. The arrows indicate (1) generation of near surface turbulence through direct wind shear (shear instability), (2) generation of wind waves, (3) increase of surface drag (wind stress), (4) turbulence generation by wind waves, (5) enhanced dissipation of wind waves by near subsurface turbulence, (6) enhanced viscous dissipation of wind waves, (7) break up and accumulation of surface films by waves, (8) suppression of near surface turbulence by modified surface boundary conditions, (9) break up and accumulation of surface films by near surface turbulence, (10) generation of bubbles by wave breaking, (11) gas exchange due to bubbles, (12) gas exchange due to wave motion, (13) gas exchange due to near surface turbu-

[1]Now at Interdisciplinary Center for Scientific Computing, University of Heidelberg, Germany.

Paper number 1999JC900200.
0148-0227/99/1999JC900200$09.00

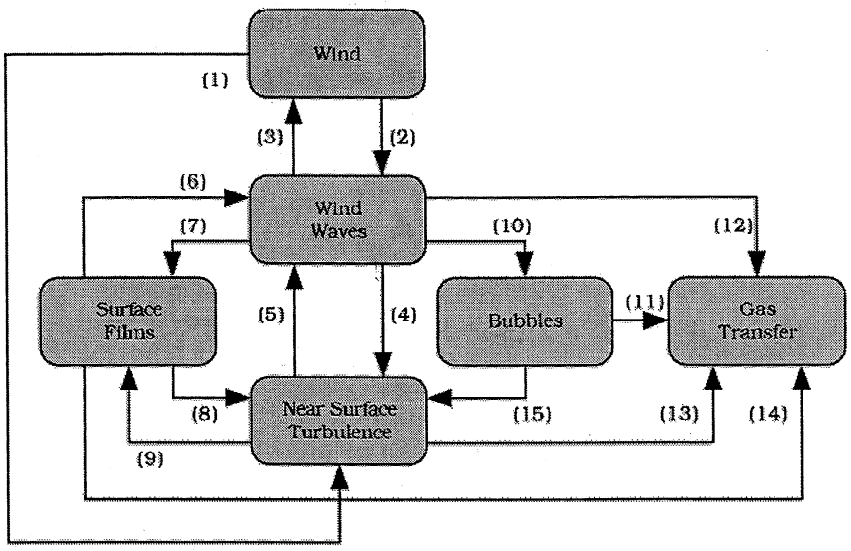

Figure 1. Physical processes influencing air-sea gas exchange.

lence, (14) suppression of gas exchange by surface films (barrier to diffusion), and (15) enhancement of turbulence by bubbles.

It is clear that all the physical processes in Figure 1 may influence the air-sea gas transfer either directly or indirectly. Therefore the parameterization of the transfer velocity should, in principle, incorporate all these processes. It is particularly noteworthy that there are no direct effects of wind on the gas exchange. Wind may only influence the surface waves and the near surface turbulence which directly control the exchange process.

A few theoretical models have been proposed which address influences of surface waves on the air-sea gas exchange. Both *Coantic* [1986] and *Back and McCready* [1988] suggest that the wave orbital motion of nonbreaking gravity-capillary waves may be responsible for the enhancement of the gas transfer velocity. However, *Csanady*'s [1990] model suggests that surface convergence/divergence generated at the crests of short gravity waves during microscale breaking is the most effective mechanism of air-sea gas exchange.

In addition to these effects, surface waves may enhance near-surface turbulence (eddy motions not directly associated with wave orbital motions) and hence may increase the air-sea gas exchange. Recent field studies have shown that the turbulence dissipation rate within a few meters below the air-sea interface is significantly higher than the typical value associated with shear-induced turbulence at high wind speeds [*Agrawal et al.*, 1992; *Drennan et al.*, 1995; *Terray et al.* 1995]. The recent studies argue that intermittent large breaking events are responsible for the increase of the overall turbulence level. During our recent field investigation off the California coast, we have found that the turbulence level within 0.2-0.4 m from the surface can be much higher than that of shear-induced turbulence even without the presence of large breaking waves [*Bock et al.*, 1995]. We suspect that turbulence very close to the air-sea interface can be generated by smaller surface waves either by breaking or as a result of wind-wave interaction (generation of longitudinal eddies). The latter has been reported in a recent laboratory experiment by *Melville et al.* [1998] and in a field observation by *Gemmrich and Hasse* [1992]. Whatever the dominant mechanism may be, surface waves are most likely responsible for the enhancement of near-surface turbulence in a wide range of wind conditions.

In this study we focus on the relationship between wind-generated waves and air-sea transfer of weakly soluble, nonreactive gases over clean water surfaces as well as in the presence of surface films. Only conditions at low to medium wind speeds are considered since we do not include the effect of bubbles on gas exchange in the analyses. *Jähne et al.* [1987] has suggested that there is an unambiguous correlation between the total mean square slope of wind waves and the gas-transfer velocity. This conclusion has been derived from experimental data collected in three very different wind-wave flumes. However, our recent laboratory study [*Hara et al.*, 1995] shows that the gas transfer velocity shows a strong correlation with very short wind waves (wavenumber above 200 rad/m) but a very weak dependence on longer waves (wavenumber less than 100 rad/m). Here we report results from our measurements of gas-transfer across very clean air-water interfaces as well as interfaces with artificial surfactant. Since surface films tend to suppress shorter gravity-capillary waves with little effect on gravity waves, they are useful in determining the scale of waves which are most important for the air-sea gas exchange process. The application of a scanning laser slope gauge (SLSG) enables us to examine the wind-generated wave field in detail.

2. Experimental Method

Experiments were performed in two annular tanks of very different scales. The first experiment took place at Woods Hole Oceanographic Institution (WHOI) in a small annular polycarbonate channel (0.25 m mean radius, 0.1 m width, 0.1 m depth) with a gas-tight airspace to allow both gas invasion and evasion experiments. The geometry of the tank is very similar to that used by *Jähne et al.* [1987] during their small tank experiments. Our tank had multiple ports for air phase purging, for sampling of both liquid and gas phases, and for surface skimming to remove surface films. Wind-driven waves were generated by a disc with rows of vertical vanes arranged around the disc perimeter. Instrumentation in this wave tank included a fixed-point laser slope gauge, a current meter, an oxygen probe, and a surface tension electrobalance. The laser slope gauge allowed point measurements of wave slope spectra in the tank with a Nyquist frequency of 150 Hz (sampling frequency of 300 Hz). Wind stress was estimated by the momentum balance method [*Jähne et al.*, 1984]. Gas transfer velocities were derived from measurement of the evasive flux of O_2 using a Strathkelvin oxygen probe mounted at 0.05 m height in the annular channel; the probe tip extended 0.03 m laterally into the channel. The probe was calibrated using oxygen-free water and air as standards and corrected for sensitivity to temperature. An oxygen-free atmosphere was maintained in the tank headspace by continuous purging with humidity- and temperature-conditioned zero grade N_2. The loss of oxygen from the aqueous phase was monitored continuously, sampling at 1 Hz. The response time of the electrode was of the order of 1 s, while the mixing time of the tank was less than 1 min. Transfer velocities were calculated for one min intervals from the O_2 flux using the standard flux equation. During clean water experiments, we carefully cleaned the tank after each experiment and tried different sources of water including local tap water, distilled water generated from local tap water, and commercially available spring water from two different sources. We found that only spring water from a particular source was sufficiently clean, that is, the gas exchange measurements were repeatable and yielded consistently high values. To study the influence of surfactant on the gas exchange, Triton X100 at a fixed concentration (0.1 μM/L) was used.

The second experiments were performed in an annular tank at the University of Heidelberg (UH) (2 m mean radius, 0.3 m width, 0.25 m depth), which was equipped with a rotating paddle ring for wind generation and a degassing unit [*Schmundt et al.*, 1995]. This tank was also used by *Jähne et al.* [1987] during their large circular tank experiments. Gas transfer velocities were determined by methods similar to those used in the small tank except that the invasive flux of O_2 was measured. Prior to each tank run, the aqueous phase was degassed under vacuum using a hollow fiber membrane unit to reduce O_2 concentrations to about 10% of the equilibrium value. Invasion of O_2 from the air in the headspace was then monitored during the experiment using two temperature-compensated oxygen probes, one mounted at middepth (0.125 m) on the channel sidewall and one at the tank bottom in a bypass of the water circulation system. The mixing time of the large tank was 3-4 min. Estimates of transfer velocity were made over 5 min intervals. In addition, measurements of sulfur hexafluoride (SF_6) evasion were made by spiking aliquots of sulfur hexafluoride enriched water into the aqueous phase prior to each run and monitoring the decrease in SF_6 concentration using gas chromatography with electron capture detection [*Wanninkhof et al.*, 1991]. Estimates of gas transfer velocity by the two methods generally agreed to within $\pm 15\%$. (Only the O_2 invasion flux data are shown in this study.) The conversion of the measured transfer velocity to that at Schmidt number 600 (k_{600}) was made assuming that the transfer velocity was proportional to $S_c^{-1/2}$, since the water surface was covered by waves in all experimental cases. Wind stress was estimated by the momentum balance method [*Jähne et al.*, 1984]. In addition, mean wind speed was monitored at 0.3 m height above the mean water surface using a propeller anemometer. Wind waves were measured using a scanning laser slope gauge developed by *Bock and Hara* [1995]. The instrument was capable of measuring the three-dimensional wavenumber-frequency slope spectrum of capillary-gravity waves for wavenumbers between 30 and 1200 rad/m with a Nyquist frequency of 20.8 Hz. The instrument was successfully tested in a laboratory experiment, and the associated instrumental errors were fully analyzed [*Bock and Hara*, 1995].

Different concentrations of surfactant (Triton X100) were used to study their effect on surface waves and on air-water gas exchange. In order to keep the water surface free from contamination other than artificially added surfactant, the surface was continuously skimmed during the experiment. Visual observations confirmed that the presence of the skimmer did not affect the wind wave field. The surface skimming effectively eliminated any surface films due to insoluble (hydrophobic) surfactant which existed in the tank. Only soluble (hydrophilic) surfactant, such as Triton X100, still influenced the surface rheology and hence surface waves and air-water gas transfer. During the course of experiments with clean water, water samples were drawn into a small linear tank. Surface tension was measured with a Cahn 2000 electrobalance and a platinum Wilhelmy plate, and mechanically generated capillary-gravity waves were used to measure the surface viscoelasticity. We ascertained that the surface tension was close to the theoretical value (0.073 N/m at 20°C) and the surface viscoelasticity was negligibly small. This test confirmed that our experiments were not significantly influenced by surfactant which natu-

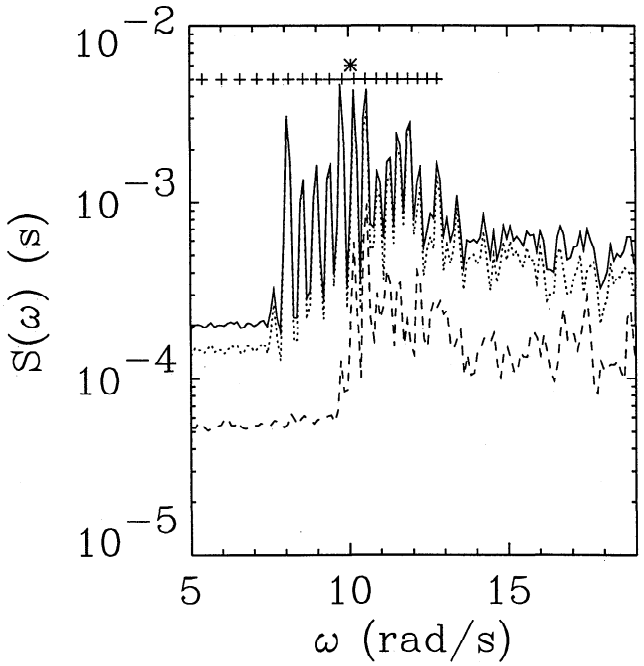

Figure 2. Frequency slope spectrum of surface waves. Run number 2. Solid line indicates total slope spectrum; dotted line indicates along-tank slope spectrum; dashed line shows cross-tank slope spectrum; pluses show frequencies of lowest 25 along-tank wave modes; star shows frequency of lowest cross-wave tank mode.

rally existed in the tank and that any observed surfactant effects were due to the added Triton X100.

3. Results of Wave Field Measurements

First we report the detailed wave field observed in the circular tank at UH. In Figure 2 we show typical frequency spectra of along-tank slope, cross-tank slope, and total slope in a lower frequency range. These results have been obtained at a wind friction velocity of 0.42 m/s and with clean water. One immediately notices that the along-tank slope spectrum suddenly increases above the noise level at a certain frequency (we call it threshold frequency). For the case of Figure 2 the threshold frequency is about 8 rad/s. Above the threshold frequency the along-tank slope spectrum shows successive discrete peaks. The locations of these peaks correspond to the frequencies of along-tank wave modes allowable in this particular tank geometry. For a given constant (along-tank) current velocity we may calculate the frequencies of the along-tank wave modes, i.e., waves whose wavelengths are 1/1, 1/2, 1/3, 1/4, ... of the circumference of the tank, using the theoretical dispersion relation. After some iterations we have found that the mean current velocity can be determined uniquely and very precisely (within an error of $\pm$ 0.002 m/s) by optimizing the agreement between the observed spectral peaks and the calculated frequencies. In Figure 2 the calculated frequencies of the lowest 25 modes are indicated by crosses. The agreement with the observed peaks is excellent for a wide range of frequency.

Another noticeable feature of the slope spectra is that the cross-tank slope also increases above a certain frequency (about 10 Hz in Figure 2). This frequency corresponds to that of the lowest cross-tank wave mode allowed in the tank, which is indicated by a star in Figure 2).

Since the resolution of the wavenumber slope spectrum obtained using the scanning laser slope gauge ($S_w(k)$) is only 30 rad/m, the instrument is not suitable for measuring waves much longer than a few centimeters. However, we may obtain very accurate wavenumber slope spectra at lower wavenumbers ($S_f(k)$) by converting the frequency slope spectra ($S(\omega)$), since the relationship between frequency and wavenumber is determined unambiguously. It has been found that the two estimates of the wavenumber slope spectra overlap reasonably well between wavenumbers 25 and 125 rad/m. Therefore the complete wavenumber slope spectra may be constructed by connecting the two spectral estimates smoothly over this wavenumber range. We have accomplished this by linearly varying the relative weight of each contribution between 0 and 1:

$$S(k) = \frac{k-25}{100} S_w(k) + \frac{125-k}{100} S_f(k), \quad 25 < k < 125(\text{rad/m}). \quad (1)$$

Such results are shown in Figure 3 for various wind and surfactant conditions. We plot the degree of saturation $B(k) = k^2 S(k)$ (for precise definitions see the appendix) instead of the slope spectrum $S(k)$, since $B(k)$ remains in the same order of magnitude for the entire wavenumber range. The numbers in Figure 3 indicate the run numbers referred to in Table 1. Note that the spectra in Figure 3 have been smoothed for visual ease, so that discrete peaks are not observed at lower wavenumbers. For each experimental run, we have summarized the wind friction velocity, the wind speed at 0.3 m height, the threshold wavenumber (converted from the threshold frequency), the surfactant concentration, the mean along-tank current velocity, and the gas transfer velocity in Table 1.

We observe that longer gravity waves (wavenumber below 12 rad/m) are hardly affected by the surfactant. In fact, the threshold wavenumber monotonically decreases as the wind friction velocity increases regardless of the surfactant concentration (see Table 1). Just above the threshold wavenumber the degree of saturation seems to remain stationary near the value of 10^{-2} for all cases. At the intermediate wavenumber range (between 20 rad/m and 60 rad/m) the degree of saturation does not simply correlate with the wind friction velocity any more but is moderately reduced by surfactant. For example, the degree of saturation value of run number 10 (with surfactant) is about half that of run number 3 (with clean water) even if the wind stress

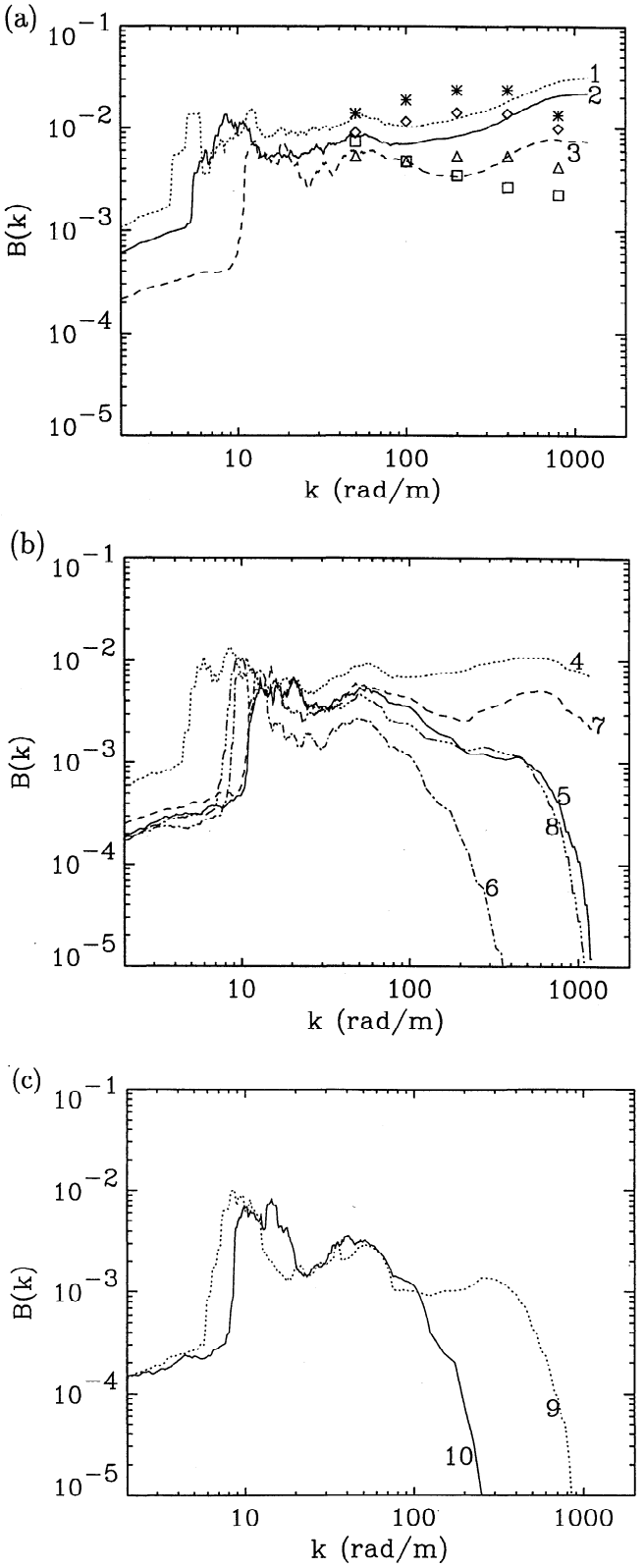

Figure 3. Degree of saturation of surface waves versus wavenumber. Numbers correspond to run numbers in Table 1. (a) Clean water is used. Different symbols are data by *Jähne and Riemer* [1990]. Stars indicate $u_* = 0.72$ m/s; diamonds indicate $u_* = 0.42$ m/s; triangles indicate $u_* = 0.27$ m/s; and squares indicate $u_* = 0.21$ m/s. (b) Triton X100 concentrations between 0.14 and 0.47 μM/L are used. (c) Triton X100 concentrations above 1.24 μM/L are used.

is slightly higher. At higher wavenumbers (above 100 rad/m), surfactant shows significant influence on waves. In two cases (run numbers 6 and 10), waves above 200-300 rad/m are completely eliminated. In three other cases (run numbers 5, 8, and 9), waves are strongly suppressed above 800-1000 rad/m. However, the clean water results remain high up to the maximum resolvable wavenumber of 1200 rad/m. We also notice that the bulk concentration of Triton X100 is not a perfect parameter to describe the surface film condition if we compare the run numbers 5 and 6. Although the surfactant concentration and the wind stress are similar in both cases, the wave fields are very different.

Our results for clean water cases can be compared with previous study in a large linear wind wave flume at a 100 m fetch by *Jähne and Riemer* [1990], shown by different symbols in Figure 3a. Although our spectral values around 50-100 rad/m are consistent with or slightly lower than those by *Jähne and Riemer* [1990], our results at higher wavenumbers are consistently higher. In the large linear facility the degree of saturation decreases rapidly above wavenumber 800 rad/m or so. However, our results in the circular tank do not show such a trend. It is not clear whether the discrepancy between the two experiments is because of the difference of the tank geometry or because of our careful cleaning of the surface.

During the WHOI experiment, wave slope measurements were performed at a fixed point only. Therefore we may calculate the total mean square slope and the frequency wave slope spectrum. By estimating the mean current velocity as described above, the frequency spectrum can be converted to the wavenumber slope spectrum at lower wavenumbers. Since the scale of the largest waves in the WHOI tank is smaller than that in the UH tank by at least a factor of 2, we assume that our estimated wavenumber slope spectra are accurate up to wavenumber 200 rad/m (compared to 125 rad/m in the UH tank) in later analyses. Above this wavenumber the frequency slope spectrum is likely to be affected by the Doppler shift due to orbital velocities of longer waves.

In Figure 4 we plot the total mean square slope versus the wind friction velocity from our experiments at UH and WHOI as well as from previous laboratory experiments by *Jähne et al.* [1987] and *Hara et al.* [1997]. Our clean water results (open squares and open diamonds) are consistent with the circular tank results by *Jähne et al.* [1987] (crosses and pluses), except that at high friction velocities our results are lower. These circular tank results are also similar to the large linear tank results at a 40 m fetch by *Jähne et al.* [1987], shown by triangles, for the entire friction velocity range. However, the results from a small linear tank at a 13 m fetch by *Hara et al.* [1997] are consistently lower at all friction velocities. *Jähne et al.* [1987] speculates that the good agreement of the total mean square slope between the

Table 1. Experimental Parameters in Large Circular Tank

Run Number	u_*, m/s	U(0.3 m), m/s	Threshold Wavenumber, rad/m	Triton X100 Concentration, μM/L	Mean Current, m/s	Mean Square Slope	$k_{600} \times 10^5$, m/s
1	0.57	7.5	4.5	0	0.215	0.074	11.2
2	0.42	5.5	6.0	0	0.140	0.049	6.6
3	0.23	3.5	11.0	0	0.089	0.022	3.6
4	0.46	7.5	5.0	0.42	0.165	0.046	5.4
5	0.29	5.5	8.5	0.47	0.105	0.0181	2.8
6	0.25	5.5	9.5	0.47	0.094	0.0110	1.39
7	0.21	3.5	11.5	0.14	0.086	0.022	2.7
8	0.19	3.5	12.0	0.34	0.081	0.0170	1.89
9	0.37	7.5	6.5	1.24	0.122	0.0139	3.1
10	0.28	5.5	9.0	1.44	0.099	0.0124	1.92
11	0.15	3.5	?	1.97	?	?	1.19

large linear tank and the circular tanks is coincidental because the wave fields look very different. Specifically, dominant fetch-dependent gravity waves are present in the linear tank, while no dominant waves are present in the circular tanks. Combined with our short fetch results, it may be reasonable to conclude that the total mean square slope increases with fetch at a given wind stress in linear tanks and that the circular tanks happen to yield mean square slope values similar to those in the linear tank with a 40 m fetch. This conclusion is further supported by our recent field observations with almost unlimited fetch. It has been found that typical total mean square slope values are roughly 2 (higher wind) to 10 (lower wind) times larger than the circular tank results for a given wind stress [*Hara et al.*, 1998]. Finally, the results with surfactant yield consistently lower mean square slope values as expected.

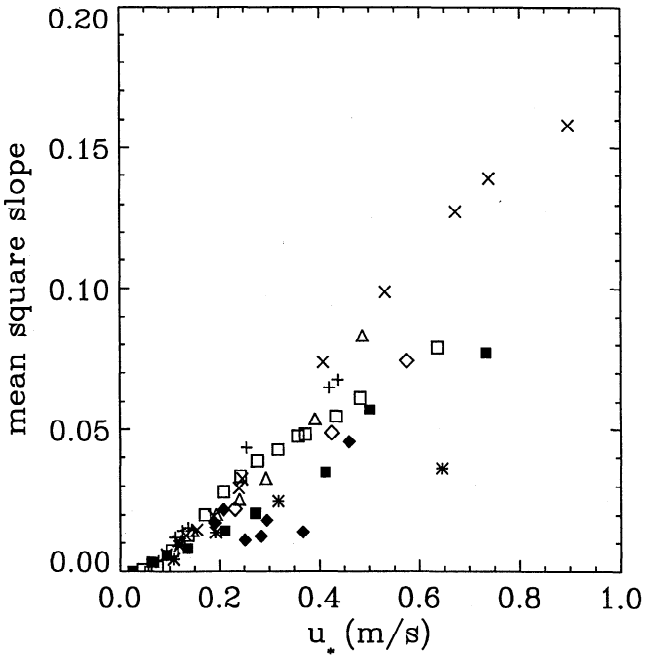

Figure 4. Total mean square slope of surface waves versus wind friction velocity. Open squares indicate small circular tank with clean water, from this study; filled squares indicate small circular tank with surfactant, from this study; open diamonds indicate large circular tank with clean water, from this study; filled diamonds indicate large circular tank with surfactant, from this study; pluses indicate small circular tank, [*Jähne et al.*, 1987]; crosses indicate large circular tank, [*Jähne et al.*, 1987]; triangles indicate large linear tank with 40 m fetch [*Jähne et al.*, 1987]; stars indicate small linear tank with 13 m fetch [*Hara et al.*, 1997].

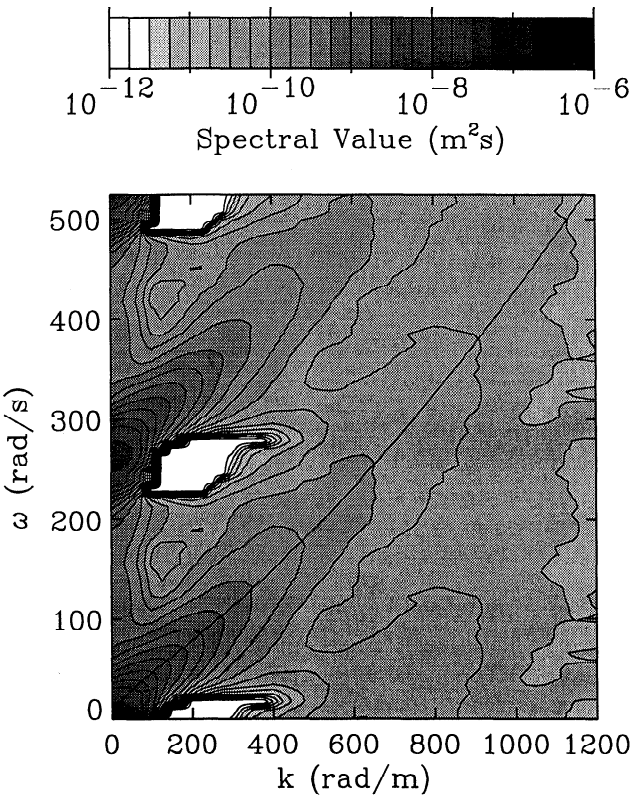

Figure 5. Frequency-wavenumber slope spectrum of surface waves. Along-tank direction. Run number 2. Solid line shows theoretical dispersion relation including bulk mean current.

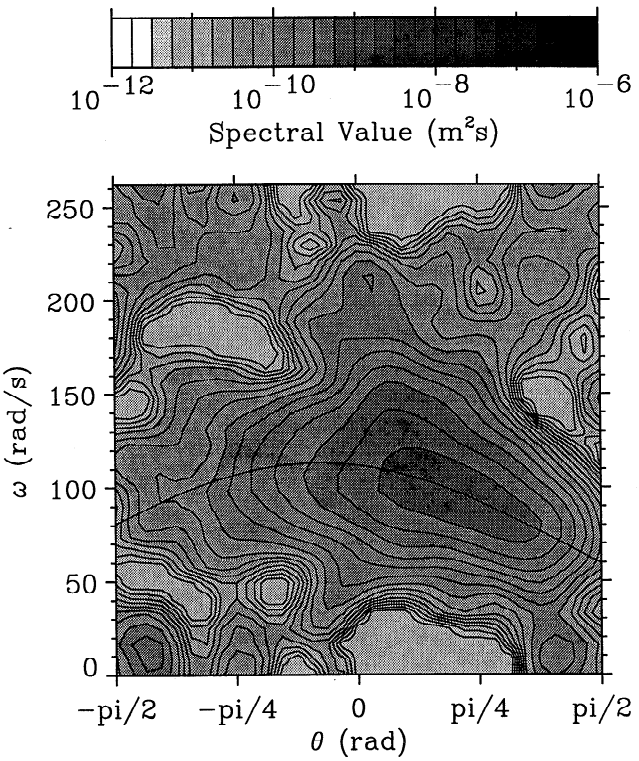

Figure 6. Directional frequency slope spectrum of surface waves. Wavenumber 300 rad/m. Run number 2. Solid line shows theoretical dispersion relation including bulk mean current.

In Figure 5 we show the one-sided wavenumber-frequency slope spectrum (see the appendix for definition) along the wind direction for a clean water case obtained at the UH circular tank (run number 2). Note that the frequency range of Figure 5 is 4 times the Nyquist frequency so that the upper half of Figure 5 is identical to the lower half. The solid line is the dispersion relation of gravity-capillary waves including the Doppler shift by the along-tank current. Since the along-tank current velocity has been estimated by matching the observed and calculated frequencies of the longest several wave modes of the tank, this value should correspond to the bulk current rather than the near-surface current. In Figure 5 the wave energy is observed to be mostly concentrated along the dispersion relation up to wavenumber 900 rad/m. This fact suggests that most of the waves are propagating freely at their own phase speed and that the along-tank current is nearly uniform up to the vicinity of the surface (except possibly within 1 mm of the surface). The former characteristic is very different from that reported by *Hara et al.* [1997] in a fetch-limited linear wind wave flume. It has been found that in the presence of fetch-limited dominant steep waves, a significant part of the wave energy at high wavenumbers is bound to dominant waves and propagates at the same speed as the dominant waves. Since the circular tank geometry does not allow excitation of steep dominant gravity waves, the level of the bound higher harmonics is expected to be much lower than that of freely propagating waves in Figure 5. The directional frequency slope spectrum at a fixed wavenumber (k = 300 rad/m) is shown in Figure 6 for the same case (run number 2). One immediately notices that the peak of the wave spectrum is observed around θ = 0.5-0.7 rad (30-40°); that is, the waves are propagating outward relative to the along-tank direction. This is a natural consequence of the circular tank geometry.

4. Results of Transfer Velocity

Currently, most of our estimates of the air-sea gas exchange relies on the empirical relationships between the mean wind speed and the transfer velocity [*Liss and Merlivat*, 1986; *Wanninkhof*, 1992]. However, as shown in Figure 1, the actual transfer process is mainly controlled by surface waves and near surface turbulence; the effect of wind is at most indirect. It is therefore preferable to include surface wave spectra and near surface turbulence fields in the parameterization of the transfer velocity if such information is available. Alternatively, we may be able to improve our estimates by using the wind friction velocity instead of the wind speed, since surface waves and near surface turbulence are more closely related to the wind stress than to the wind speed.

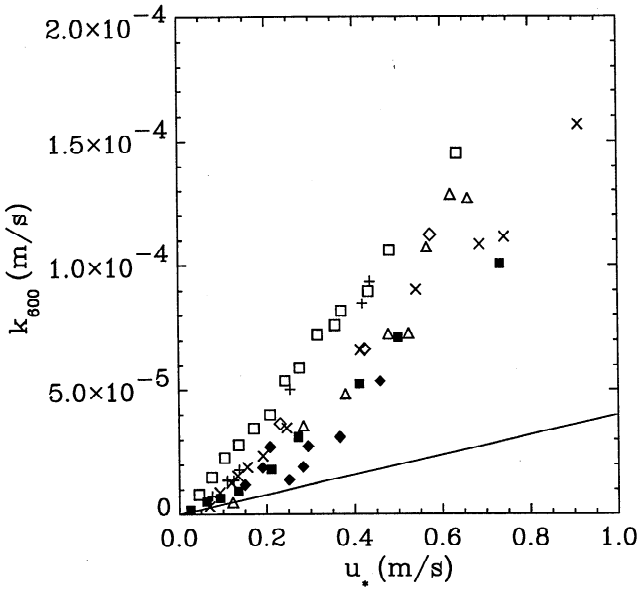

Figure 7. Gas transfer velocity versus wind friction velocity. Open squares indicate small circular tank with clean water, from this study; filled squares show small circular tank with surfactant, from this study; open diamonds indicate large circular tank with clean water, from this study; filled diamonds indicate large circular tank with surfactant, from this study; pluses show small circular tank, [*Jähne et al.*, 1987]; crosses show large circular tank, [*Jähne et al.*, 1987]; and triangles show large linear tank with 40 m fetch [*Jähne et al.*, 1987]. Solid line is transfer velocity under a smooth surface proposed by *Deacon* [1977].

In Figure 7 we plot the transfer velocity versus the wind friction velocity from this study as well as from previous studies in different wind wave flumes. The results with clean water from the large circular tank (open diamonds and crosses) and those from the linear tank with a 40 m fetch (triangles) exhibit a reasonable correlation with the friction velocity. The transfer velocity increases slightly faster than linearly with the friction velocity. The results from the small circular tanks (open squares and pluses) are slightly higher than the other results at higher wind stresses. Our small circular tank results (open squares) alone are strictly linear with friction velocity and, at lower wind stresses, are significantly higher than the rest of the results including the small circular tank results by *Jähne et al.* [1987]. This is because of our careful cleaning of the tank and selection of very clean water. Once surfactant is introduced the transfer velocity decreases significantly even at moderate friction velocities. For reference we also show the transfer velocity under a smooth surface by a solid line. This line is calculated based on the formulation proposed by *Deacon* [1977]:

$$k_s = 0.082(\rho_a/\rho_w)^{1/2} S_c^{-2/3} u_* \qquad (2)$$

where k_s is the transfer velocity under a smooth surface, ρ_a is the air density, ρ_w is the water density, and S_c is the Schmidt number (S_c = 600 in Figure 7). Even with surface films, all of our results are larger than the smooth surface value. This is consistent with the fact that we observed surface waves in all cases.

In Figure 8 we report our results of the gas transfer velocity against the wind speed measured at 0.3 m height obtained from the large circular tank at UH. As expected, the relationship between the wind speed and the transfer velocity is very poor once the surfactant is introduced. The transfer velocity may decrease by as much as 80% for a given wind speed.

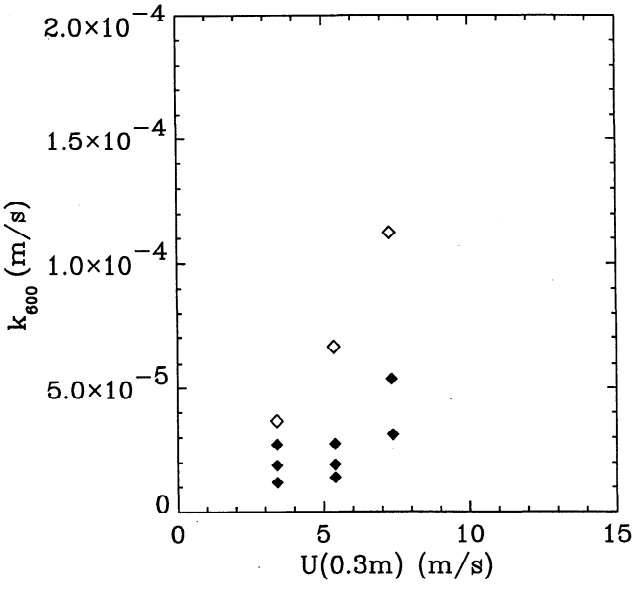

Figure 8. Gas transfer velocity versus wind speed measured at 0.3 m height. Open diamonds indicate large circular tank with clean water; filled diamonds indicate large circular tank with surfactant.

The correlation is somewhat improved if the friction velocity is used instead of the wind speed as in Figure 7 (see solid and empty diamonds). This is because the surfactant reduces the friction velocity at a given wind speed, by decreasing the form drag due to short wind waves. Still, the parameterization based on the wind friction velocity alone exhibits reduction of the transfer velocity by up to 60% in the presence of surface films. These observations suggest that wind stress alone is not sufficient to characterize the physical processes which control gas transfer in the presence of surface films [*Frew et al.*, 1995].

Next, in Figure 9a, the gas transfer velocity is plotted against the total mean square slope for all of our results (large and small circular flumes, with and without surface films). We notice that the total mean square slope shows a reasonable linear correlation with the transfer velocity regardless of the surfactant concentrations, being consistent with the observation by *Jähne et al.* [1987]. A simple linear fit to our observations is also shown in Figure 9. The root mean square error of our data from the linear fit is only 8.6×10^{-6} m/s. However, the same linear relationship is not likely to hold in larger wind wave flumes or in open ocean conditions since the total mean square slope is significantly higher due to contributions from longer gravity waves. In Figures 9b-9d the transfer velocity is shown against the mean square slope integrated over certain wavenumber ranges. Figure 9b shows a poor correlation between the transfer velocity and the mean square slope of larger waves. The root mean square error from the linear fit is 2.8×10^{-5} m/s. This observation suggests that larger waves are not directly related to the gas exchange process. As the scale of the waves decreases to wavenumbers between 50 and 200 rad/m (Figure 9c), the correlation seems to improve slightly (the root mean square error from the linear fit is 2.0×10^{-5} m/s). The mean square slope of very short waves (wavenumber above 200 rad/m) shows a reasonable linear correlation with the transfer velocity (Figure 9d). The root mean square error decreases to 1.0×10^{-5} m/s, which is almost as small as that of Figure 9a. On the basis of these observations, we may speculate that short wind waves (wavelength less than a few centimeters) make an important contribution to the gas transfer process. It also implies that the spectral level of shorter wind waves is a good parameter in estimating the gas transfer velocity as long as the spectral level is moderate to high. At very low spectral values the correlation between transfer velocity and short wind waves is rather poor, suggesting that turbulence unrelated to surface waves may become important for gas exchange under such conditions.

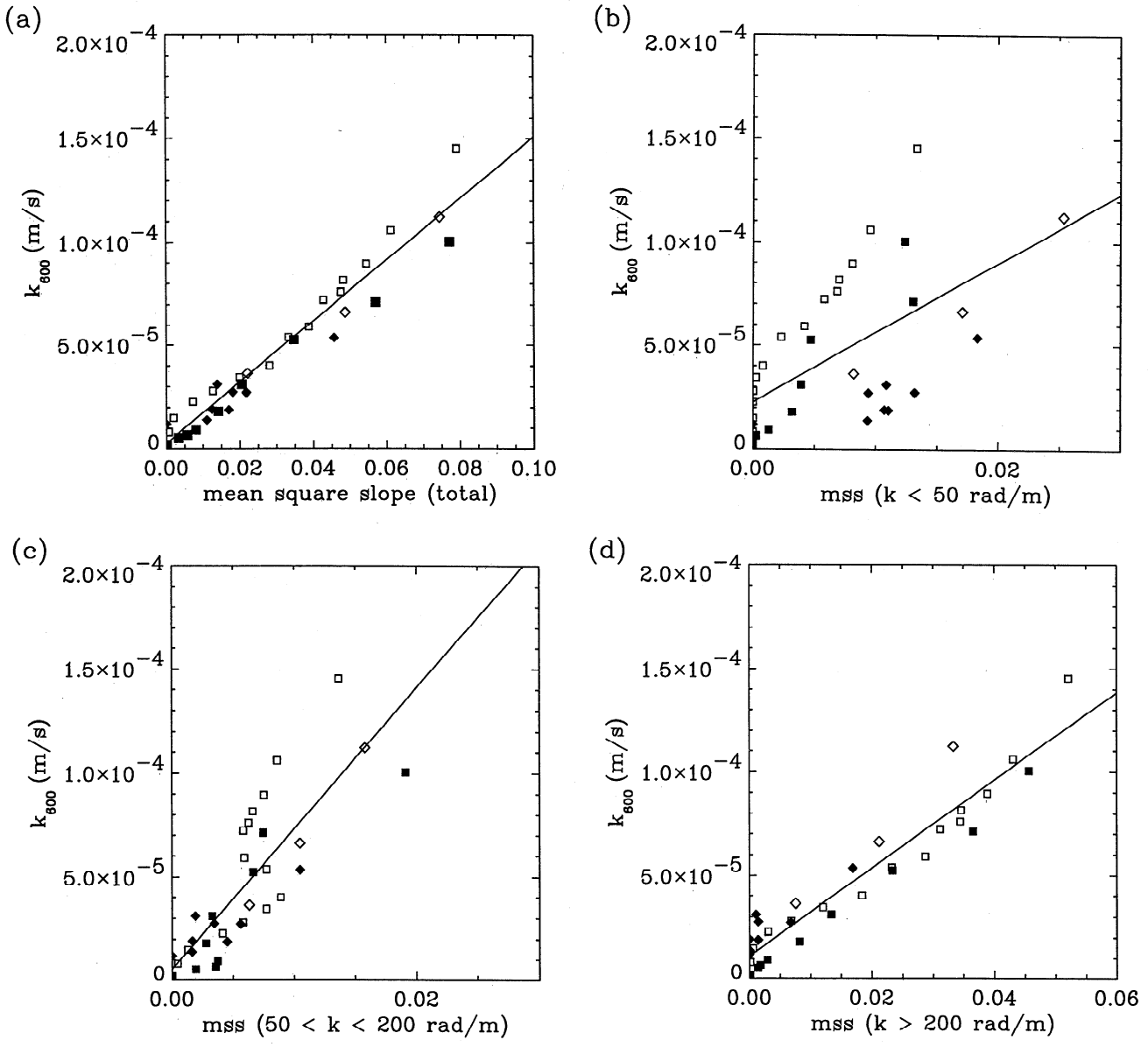

Figure 9. Gas transfer velocity versus mean square slope. Open squares indicate small circular tank with clean water; filled squares indicate small circular tank with surfactant; open diamonds show large circular tank with clean water; filled diamonds show large circular tank with surfactant. The solid line is the best linear fit to the observation. The mean square slope is calculated over (a) all wavenumbers, (b) wavenumber below 50 rad/m, (c) wavenumber between 50 and 200 rad/m, and (d) wavenumber above 200 rad/m.

Jähne et al. [1987] concluded that the gas transfer velocity was more closely related to the total mean square slope than the mean square slope of short wind waves. This conclusion was derived from their observations when the wind speed was changed periodically between 5.4 and 2.7 m/s. The response of the gas transfer velocity to the changing wind was similar to that of the total mean square slope rather than that of the mean square slope of short wind waves only. In fact, we also observe that the transfer velocity correlates slightly better with the total mean square slope than with the mean square slope of short wind waves only. However, the poor relationship between the transfer velocity of longer wind waves and the transfer velocity (in particular, in the presence of surface films) in Figure 9b leads us to believe that longer waves are not directly related to the gas transfer process.

With our limited data it is not feasible to draw any conclusions regarding the physical processes of the gas transfer related to short wind waves. However, we may comment on some of the previous studies based on our experimental results. *Csanady* [1990] has proposed that microscale breaking of short gravity waves is responsible for the gas exchange. Recent theoretical studies

[e.g., *Longuet-Higgins*, 1995] suggest that short gravity waves of order 0.1 m may produce parasitic capillaries on the forward face of the crest accompanied by a region of high vorticity, being consistent with laboratory observations by *Okuda* [1982]. *Jessup et al.* [1997] has identified regions of surface renewal due to microscale breaking of short wind waves (wave length roughly 0.1-0.5 m) using an infrared imagery technique both in laboratories and in situ. All these studies suggest the possible importance of short gravity waves in gas exchange. Our results, however, do not show a strong correlation between waves of the comparable scale and the transfer velocity (see, e.g., Figure 9c). Of course, this does not necessarily imply that microscale breaking is not important for gas exchange. While the spectral level of short wind waves in the range of 0.1-0.5 m is affected by surface films only weakly, the occurrence of microscale breaking and resulting surface renewal can be significantly reduced in the presence of surface films. Such effects are not reflected in our simple correlation studies.

5. Concluding Remarks

We have conducted laboratory studies on the relationship between air-sea exchange of weakly soluble, nonreactive gases and wind generated waves, with clean water as well as with artificial surfactant. Only low to medium wind speeds have been considered where the effects of bubble formation and air entrainment are not significant. Our detailed study of the structure of surface waves in a circular wind wave flume has revealed significant differences from that in a fetch-limited linear tank.

The correlation between the wind speed and the transfer velocity is poor in the presence of surface films. The correlation is somewhat improved if the wind stress is used instead of the wind speed. Still, the transfer velocity may decrease by up to 60% due to surfactant at a given wind stress. The transfer velocity shows a linear correlation with the total mean square slope as reported by *Jähne et al.* [1987]. While the transfer velocity poorly correlates with the mean square slope of large waves (wavenumber below 50 rad/m), it shows reasonable correlation with short wind waves (wavenumber above 200 rad/m). These observations imply the significance of short wind waves in the gas transfer process.

Although our parametric study may be useful in estimating the relative significance of different surface wave components in the air-sea gas exchange, the detailed transfer process cannot be addressed unless the surface renewal caused by waves and turbulence is directly investigated. Combination of the observation of surface renewal (using infrared techniques) and the measurements of relevant physical processes, including wind, waves, subsurface turbulence, surface films, and bubbles, may be a necessary step toward a better understanding of the air-sea gas exchange process.

Appendix: Definition of Surface Wave Slope Spectrum

Let us define a coordinate system such that the x axis is in the mean wind direction, the z axis is vertically upward measured from the mean water surface, and the y axis is defined according to the right-hand rule. We denote the surface elevation by $z = \zeta(x, y, t)$ and the surface slope by $\nabla\zeta = (\partial\zeta/\partial x, \partial\zeta/\partial y)$. The autocorrelation function of the surface slope is defined as

$$R(\xi, \eta, \tau) = \overline{\nabla\zeta(x, y, t) \cdot \nabla\zeta(x + \xi, y + \eta, t + \tau)} \quad \text{(A1)}$$

where the overbar indicates the time average. Then the three-dimensional one-sided frequency-wavenumber slope spectrum is calculated to be

$$S(k, \theta, \omega) = \frac{1}{4\pi^3} \iiint_{-\infty}^{\infty} e^{-i(k\xi\cos\theta + k\eta\sin\theta - \omega\tau)} \times R(\xi, \eta, \tau) d\xi\, d\eta\, d\tau \quad \text{(A2)}$$

where k is the wavenumber, ω is the angular frequency, and θ is the wave direction measured from the x axis in the counterclockwise direction. Here $\theta = 0$ corresponds to waves in the wind direction and $\theta = \pm\pi/2$ corresponds to waves in the crosswind directions. This three-dimensional spectrum is defined for $0 < k < \infty$, $-\infty < \omega < \infty$, and $-\pi/2 < \theta < \pi/2$. Note that a negative ω corresponds to waves propagating against the wind. By definition, the mean square slope is recovered by integrating $S(k, \theta, \omega)$ as

$$\overline{\nabla\zeta \cdot \nabla\zeta} = \int_{-\infty}^{\infty} \int_{-\frac{\pi}{2}}^{\frac{\pi}{2}} \int_{0}^{\infty} S(k, \theta, \omega)\, k\, dk\, d\theta\, d\omega \quad \text{(A3)}$$

The one-sided, two-dimensional wavenumber spectrum is calculated by integrating $S(k, \theta, \omega)$ in frequency

$$S(k, \theta) = \int_{-\infty}^{\infty} S(k, \theta, \omega) d\omega \quad \text{(A4)}$$

which is defined for $0 < k < \infty$ and $-\pi/2 < \theta < \pi/2$. The nondimensional degree of saturation is defined as

$$B(k, \theta) = k^2 S(k, \theta) \quad \text{(A5)}$$

Finally, the omnidirectional (one-dimensional) wavenumber slope spectrum and the omnidirectional degree of saturation are defined as

$$S(k) = \int_{-\frac{\pi}{2}}^{\frac{\pi}{2}} S(k, \theta) d\theta \quad \text{(A6)}$$

and

$$B(k) = k^2 S(k) \quad \text{(A7)}$$

respectively.

Acknowledgments. We thank Bernd Jähne for his hospitality during the experiments at UH. This work was supported by U.S. National Science Foundation, Grant OCE9301334. This is WHOI contribution 10006.

References

Agrawal, Y. C., E. A. Terray, M. A. Donelan, P. A. Hwang, A. J. Williams III, W. M. Drennan, K. K. Kahma, and S. A. Kitaigorodskii, Enhanced dissipation of kinetic energy beneath surface waves, *Nature, 359*, 219-220, 1992.

Back, D. D., and M. J. McCready, Effect of small-wavelength waves on gas-transfer across the ocean surface, *J. Geophys. Res., 93*, 5143-5152, 1988.

Bock, E. J., and T. Hara, Optical measurements of capillary-gravity wave spectra using a scanning laser slope gauge, *J. Atmos. Oceanic Technol., 12*, 395-403, 1995.

Bock, E. J., et al., Description of the science plan for the April 1995 CoOP experiment, "Gas Transfer in Coastal Waters," performed from the Research Vessel New Horizon, in *Air-Water Gas Transfer*, edited by B. Jähne and E. C. Monahan, pp. 801-810, Aeon-Verlag, Hanau, Germany, 1995.

Coantic, M., A model of gas-transfer across air-water interfaces with capillary waves, *J. Geophys. Res., 91*, 3925-3943, 1986.

Csanady, G. T., The role of breaking wavelets in air-sea gas-transfer, *J. Geophys. Res., 95*, 749-759, 1990.

Deacon, E. L., Gas transfer to and across an air-water interface, *Tellus, 29*, 363-374, 1977.

Drennan, W. M., M. A. Donelan, E. A. Terray, and K. B. Katsaros, Oceanic turbulence dissipation measurements in SWADE, *J. Phys. Oceanogr., 26*, 808-815, 1996.

Frew, N., E. Bock, W. McGillis, and T. Hara, Parameterization of air-water gas transfer using wind stress and viscoelasticity, in *Air-Water Gas Transfer*, edited by B. Jähne and E. C. Monahan, pp. 529-542, Aeon-Verlag, Hanau, Germany, 1995.

Gemmrich, J., and L. Hasse, Small-scale surface streaming under natural conditions as effective in air-sea gas exchange, *Tellus, Ser. B, 44*, 150-159, 1992.

Hara, T., E. J. Bock, N. M. Frew, and W. R. McGillis, Relationship between air-sea gas transfer velocity and surface roughness, in *Air-Water Gas Transfer*, edited by B. Jähne and E. C. Monahan, pp. 611-616, Aeon-Verlag, Hanau, Germany, 1995.

Hara, T., E. J. Bock, and M. Donelan, Frequency-wavenumber spectrum of wind-generated gravity-capillary waves, *J. Geophys. Res., 102*, 1061-1072, 1997.

Hara, T, E. J. Bock, J. B. Edson, and W. R. McGillis, Observations of short wind waves in coastal waters, *J. Phys. Oceanogr., 28*, 1425-1438, 1998.

Jähne, B. K., and K. S. Riemer, Two-dimensional wave number spectra of small-scale water surface waves, *J. Geophys. Res., 95*, 11,531-11,546, 1990.

Jähne, B. K., W. Huber, A. Dutzi, T. Wais, and J. Ilmberger, Wind/wave tunnel experiments on the Schmidt number and wave field dependence of air-water gas exchange, in *Gas Transfer at Water Surfaces*, edited by W. Brutsaert and G. H. Jirka, pp. 303-309, D. Reidel, Norwell, Mass., 1984.

Jähne, B. K., K. O. Münnich, R. Bösinger, A. Dutzi, W. Huber, and P. Libner, On the parameters influencing air-water gas exchange, *J. Geophys. Res., 92*, 1937-1949, 1987.

Jessup, A. T., C. J. Zappa, and H. Yeh, Defining and quantifying microscale wave breaking with infrared imagery, *J. Geophys. Res., 102*, 23,145-23,153, 1997.

Liss, P. S., and L. Merlivat, Air-sea gas exchange rates: Introduction and synthesis, in *The Role of Air-Sea Exchange in Geochemical Cycling*, edited by P. Buat-Menard, pp. 113-127, D. Reidel, Norwell, Mass., 1986.

Longuet-Higgins, M. S., Parasitic capillary waves: A direct calculation, *J. Fluid Mech., 301*, 79-107, 1995.

Melville, W. K., R. Shear, and F. Veron, Laboratory measurements of the generation and evolution of Langmuir circulations, *J. Fluid Mech., 364*, 31-58, 1998.

Okuda, K., Internal flow structure of short wind waves, I, On the internal vorticity structure, *J. Oceanogr. Soc. Jpn., 38*, 28-42, 1982.

Schmundt, D., T. Münsterer, H. Lauer, and B. Jähne, The circular wind/wave facilities at the University of Heidelberg, in *Air-Water Gas Transfer*, edited by B. Jähne and E. C. Monahan, pp. 505-516, Aeon-Verlag, Hanau, Germany, 1995.

Terray, E. A., M. A. Donelan, Y. C. Agrawal, W. M. Drennan, K. K. Kahma, A. J. Williams III, P. A. Hwang, and S. A. Kitaigorodskii, Estimates of kinetic energy dissipation under breaking waves, *J. Phys. Oceanogr., 26*, 792-807, 1996.

Wanninkhof, R., Relationship between wind speed and gas exchange over the ocean, *J. Geophys. Res., 98*, 7373-7382, 1992.

Wanninkhof, R., J. R. Ledwell, and A. J. Watson, Analysis of sulfur hexafluoride in seawater, *J. Geophys. Res., 96*, 8733-8740, 1991.

E. J. Bock, Interdisciplinary Center for Scientific Computing (IWR), University of Heidelberg, Im Neuenheimer Feld 368, 69120 Heidelberg, Germany. (e-mail: erik@iwr.uni-heidelberg.de)

N. M. Frew and W. R. McGillis, Woods Hole Oceanographic Institution, Woods Hole, MA 02543. (e-mail: nfrew@whoi.edu; wmcgillis@whoi.edu)

T. Hara, Graduate School of Oceanography, University of Rhode Island, Narragansett, RI 02882. (e-mail: thara@uri.edu)

(Received December 10, 1997; revised January 12, 1999; accepted April 1, 1999.)